

# DEFORMABLE TEMPORAL CONVOLUTIONAL NETWORKS FOR MONAURAL NOISY REVERBERANT SPEECH SEPARATION

William Ravenscroft<sup>✉</sup>, Stefan Goetze<sup>✉</sup>, and Thomas Hain<sup>✉</sup>

Department of Computer Science, The University of Sheffield, Sheffield, United Kingdom  
{jwravenscroft1, s.goetze, t.hain}@sheffield.ac.uk

## ABSTRACT

Speech separation models are used for isolating individual speakers in many speech processing applications. Deep learning models have been shown to lead to state-of-the-art (SOTA) results on a number of speech separation benchmarks. One such class of models known as temporal convolutional networks (TCNs) has shown promising results for speech separation tasks. A limitation of these models is that they have a fixed receptive field (RF). Recent research in speech dereverberation has shown that the optimal RF of a TCN varies with the reverberation characteristics of the speech signal. In this work deformable convolution is proposed as a solution to allow TCN models to have dynamic RFs that can adapt to various reverberation times for reverberant speech separation. The proposed models are capable of achieving a 11.1 dB average scale-invariant signal-to-distortion ratio (SISDR) improvement over the input signal on the WHAMR benchmark. A relatively small deformable TCN model of 1.3M parameters is proposed which gives comparable separation performance to larger and more computationally complex models.

**Index Terms**— speech separation, deformable convolution, dynamic neural networks

## 1. INTRODUCTION

The separation of overlapping speech signals is an area that has been widely studied and which has many applications [1–3]. Deep learning models have demonstrated impressive results on separating clean speech mixtures [4, 5]. However this performance still degrades heavily under noisy reverberant conditions [6]. This performance loss can be alleviated somewhat with careful hyper-parameter optimization but a significant performance gap still exists [7].

The Conv-TasNet speech separation model has been widely studied and adapted for a number of speech enhancement tasks [4, 8–10]. Conv-TasNet generally performs very well on clean speech mixtures with a very low computational cost compared to the most performant speech separation models [5, 11, 12] on the WSJ0-2Mix benchmark [13]. As such, it is still used in many related areas of research [8, 10]. Recent research efforts in speech separation have focused on producing more resource efficient models even if they do not produce the most SOTA results on separation benchmarks [11, 12]. Previous work has investigated adaptations to Conv-TasNet with additional modifications such as multi-scale convolution and gating mechanisms applied to the outputs of convolutional layers but these significantly increase the computational complexity [14]. The Conv-TasNet model uses a sequence model

known as a TCN. It was recently shown that the optimal RF of TCNs in dereverberation models varies with reverberation time when the model size is sufficiently large [9]. Furthermore, it was shown that multi-dilation TCN models can be trained implicitly to weight differently dilated convolutional kernels to optimally focus within the RF on more or less temporal context according to the reverberation time in the data for dereverberation tasks [15], i.e. for larger reverberation times more weight was given to kernels with larger dilation factors.

In this work deformable depthwise convolutional layers [16–18] are proposed as a replacement for standard depthwise convolutional layers [4] in TCN based speech separation models for reverberant acoustic conditions. Deformable convolution allows each convolutional layer to have an adaptive RF. When used as a replacement for standard convolution in a TCN this enables the TCN to have a RF that can adapt to different reverberant conditions. Using shared weights [14] and dynamic mixing [19] are also explored as ways to reduce model size and improve performance. A PyTorch library for training deformable 1D convolutional layers as well as a Speech-Brain [20] *recipe* for reproducing results (cf. Section 5) are provided.

The remainder of the paper proceeds as follows. In Section 2 the signal model is discussed. The deformable temporal convolutional network (DTCN) is introduced in Section 3. Section 4 discusses the experimental setup, data and baseline systems. Results are given in Section 5. Section 6 provides analysis of the proposed models and conclusions are provided in Section 7.

## 2. SIGNAL MODEL

A noisy reverberant mixture of  $C$  speech signals  $s_c[i]$  for discrete sample index  $i$  convolved with room impulse responses (RIRs)  $h_c[i]$  and corrupted by an additive noise signal  $\nu[i]$  is defined as

$$x[i] = \sum_{c=1}^C h_c * s_c[i] + \nu[i] \quad (1)$$

where  $*$  is the convolution operator. The goal in this work is to estimate the direct speech signal  $s_{\text{dir},c}[i]$  and remove the reverberant reflections  $s_{\text{rev},c}[i]$  where

$$x[i] = \sum_{c=1}^C (s_{\text{dir},c}[i] + s_{\text{rev},c}[i]) + \nu[i]. \quad (2)$$

## 3. DEFORMABLE TEMPORAL CONVOLUTIONAL SEPARATION NETWORK

### 3.1. Network Architecture

The separation network uses a mask-based approach similar to [4]. The noisy reverberant microphone signal is first segmented into  $L_x$

This work was supported by the Centre for Doctoral Training in Speech and Language Technologies (SLT) and their Applications funded by UK Research and Innovation [grant number EP/S023062/1]. This work was also funded in part by 3M Health Information Systems, Inc.

blocks of length  $L_{BL}$  with a 50% overlap defined as

$$\mathbf{x}_\ell = [x[0.5(\ell-1)L_{BL}], \dots, x[0.5(1+\ell)L_{BL}-1]] \quad (3)$$

for frame  $\ell \in \{1, \dots, L_x\}$ . Motivated by [4, 5], the frames in (3) are encoded by a 1D convolutional layer with trainable weights  $\mathbf{B} \in \mathbb{R}^{L_{BL} \times N}$  such that

$$\mathbf{w}_\ell = \mathcal{H}_{enc}(\mathbf{x}_\ell \mathbf{B}) \quad (4)$$

with a rectified linear unit (ReLU) activation function  $\mathcal{H}_{enc} : \mathbb{R}^{1 \times N} \rightarrow \mathbb{R}^{1 \times N}$ . Encoded features  $\mathbf{w}_\ell$  are used as the input to a mask estimation network to produce masks  $\mathbf{m}_{\ell,c}$  for each speaker  $c \in \{1, \dots, C\}$ . The masks are then applied to the encoded features using the Hadamard product, i.e.  $\mathbf{w}_\ell \odot \mathbf{m}_{\ell,c}$  resulting in  $\mathbf{v}_{\ell,c}$ . The encoded estimate  $\mathbf{v}_{\ell,c}$  for speaker  $c$  can be decoded from the same space back into the time domain using the inverse filter of  $\mathbf{B}$ , denoted as  $\mathbf{U} \in \mathbb{R}^{N \times L_{BL}}$ , such that

$$\hat{\mathbf{s}}_{\ell,c} = \mathbf{v}_{\ell,c} \mathbf{U} \quad (5)$$

where  $\hat{\mathbf{s}}_{\ell,c}$  is the estimated clean speech signal for frame  $\ell$  in the time domain. These frames are then combined following the overlap-add method. The entire network model diagram is shown in Fig. 1.

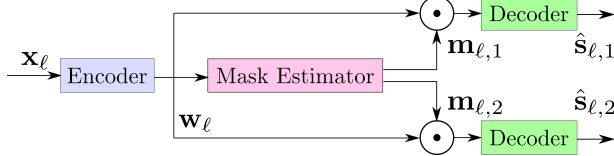


**Fig. 1:** Mask-based separation network, exemplary for 2 speakers.

### 3.2. Mask Estimation Network

In this subsection the deformable depthwise convolution (DD-Conv) layer is introduced as a replacement for depthwise convolution (D-Conv) layers and then the DTCN network is described in full. The mask estimation network consists of channelwise layer normalization (cLN) and a bottleneck pointwise convolution (P-Conv) layer which transforms the feature dimension from  $N$  to  $B$  followed by the DTCN which is followed by a P-Conv and ReLU activation to compute a sequence of masks  $\mathbf{m}_{\ell,:}$  with dimension  $C \cdot N$  [4].

#### 3.2.1. Deformable Depthwise Convolution (DD-Conv)

The formulation of DD-Conv in this section is adapted from [16] and [17]. The D-Conv operation of kernel size  $P$ , dilation factor  $f$  and convolutional kernel weights for the  $g$ th channel of an input with  $G$  channels denoted  $\mathbf{y}_g \in \mathbb{R}^{L_x}$  at the  $\ell$ th frame is defined as

$$\mathcal{D}(\ell, \mathbf{y}_g, \mathbf{k}_g) = \sum_{p=1}^P k_g[p] y_g[\ell + f \cdot (p-1)]. \quad (6)$$

The corresponding DD-Conv operator with learnable continuous offset of the  $p$ th kernel weight denoted  $\tau_{\ell,p}$  at frame  $\ell$  is defined as

$$\mathcal{C}(\ell, \mathbf{y}_g, \mathbf{k}_g, \tau_{\ell,1:P}) = \sum_{p=1}^P k_g[p] y_g[\ell + f \cdot (p-1) + \tau_{\ell,p}]. \quad (7)$$

Note that  $\tau_{\ell,p}$  only varies temporally and not across channels. It is feasible to vary these values across channels but in this work to reduce computational complexity offsets are only varied temporally.

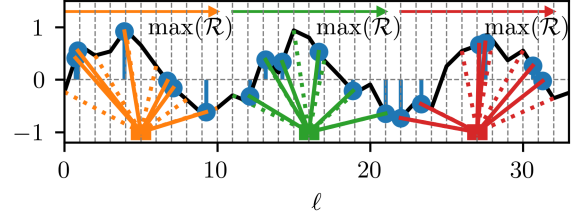


**Fig. 2:** Single channel example of Deformable depthwise convolution (bottom) on pseudo-random signal (shown in black) with a kernel size of 6, dilation factor of 2 and stride of 11.  $\mathcal{R}$  denotes the RF of the kernel. Dotted lines indicate original sampling position of kernel weights before deformation.

An illustration of the DD-Conv operation is shown in Figure 2. To simplify notation let  $\Delta\ell_p = \ell + f \cdot (p-1) + \tau_{\ell,p}$ . Linear interpolation is used to compute values of  $y[\Delta\ell_p]$  from input sequence  $y$  such that

$$y[\Delta\ell_p] = \sum_{u=\lfloor \Delta\ell_p \rfloor}^{\lfloor \Delta\ell_p \rfloor + 1} \max(0, 1 - |u - \Delta\ell_p|) y[u]. \quad (8)$$

In practice the interpolation function is designed to constrain the deformable convolutional kernel so it cannot exceed a maximum RF of  $P \cdot (f-1) + 1$  by replacing  $u = \lfloor \Delta\ell_p \rfloor$  with  $u = \min(\lfloor \Delta\ell_p \rfloor, \ell + P \cdot f - 1)$  in the bottom of the summation of (8). This constrains the kernel with the benefit of improving interpretability for the overall scope of the DTCN described in the following subsection.

#### 3.2.2. Deformable Temporal Convolutional Mask Estimation Network

The DTCN is formulated in the same way as the Conv-TasNet TCN described in [21]. This implementation deviates slightly from the original Conv-TasNet [4] by neglecting the skip connections (SCs) and associated P-Conv layers. It was found empirically that these SC layers have an negligible impact on performance ( $\leq 0.1$  dB SISDR) while having a significant negative impact on model size ( $\approx 35\%$  parameter increase).

The DTCN is composed of  $X \cdot R$  convolutional blocks where  $X, R \in \mathbb{Z}^+$  [21]. Each convolutional block consists of a P-Conv which projects the feature dimension from  $B$  to  $H$ , DD-Conv that performs a depthwise operation across the  $H$  channels and another P-Conv layer which projects the feature dimension back to  $B$  from  $H$ . The DD-Conv proceeded by P-Conv layer forms a deformable depthwise-separable convolution (DDS-Conv) structure. Depthwise-separable convolution (DS-Conv), i.e. a P-Conv proceeded by any D-Conv layer, is used as a replacement for standard convolutional layers as it is more parameter efficient and mathematically equivalent [4]. In each convolutional block the DD-Conv has an increasing dilation factor  $f$  for each additional block in a stack of  $X$  blocks as in [4, 21]. The dilation factor  $f$  increases in powers of two through the stack such that  $f \in \{1, 2, \dots, 2^{X-1}\}$ . Note that in D-Conv the dilation factor determines the fixed RF whereas in the proposed DD-Conv the dilation factor defines only the maximum possible RF of the kernel. The stack of  $X$  convolutional blocks is then repeated  $R$  times where the dilation factor is reset to 1 at the beginning of each stack. Using shared weights (SW) for each repeat is experimented with as this significantly reduces the model size similar to [14]. The offsets  $\tau_{\ell,p}$  are computed using DS-Conv following the initial P-Conv in the block, referred to as the offset sub-network. A parametric ReLU (PReLU) activation is used at the output as this allows for both negative and positive offsets. Residual connections

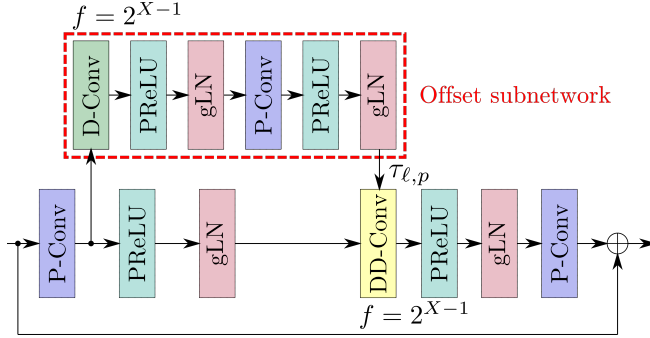


**Fig. 3:** Layers inside deformable temporal convolutional blocks.

are applied around each of the convolutional blocks similar to the TCN described in [21]. A schematic of the convolutional blocks is shown in Fig. 3.

## 4. EXPERIMENTAL SETUP

### 4.1. Data

Two datasets are used to evaluate the proposed DTCN network. The first is a clean speech mixture corpus known as WSJ0-2Mix [22]. In WSJ0-2Mix, two speech segments are overlapped at SNRs of 0 to 5 dB. The second is a noisy reverberant speech mixture corpus known as WHAMR [6]. Speech segments in WHAMR are convolved with simulated RIRs then summed together with mixing SNRs of 0 to 5 dB. Ambient noise sources from outdoor pedestrian areas are added at SNRs of -6 to 3 dB (cf. (1)). Dynamic mixing (DM), i.e. simulating new training data each epoch, is also experimented with at training time as it has been shown to lead to improved separation performance [5, 23]. Speed perturbation training is also performed as part of the DM process as described in [5].

### 4.2. Model Configuration

Feature dimensions  $N$ ,  $B$  and  $H$ , kernel size  $P$  and encoder block size  $L_{BL}$  are fixed:

$$\{N, B, H, P, L_{BL}\} = \{512, 128, 512, 3, 16\}. \quad (9)$$

These values correspond to the optimal TCN network in [4]. Note  $L_{BL}$  equates to 2 ms at 8 kHz. Five DTCN model configurations are evaluated:

$$\{X, R\} \in \{\{3, 8\}, \{4, 6\}, \{5, 5\}, \{6, 4\}, \{8, 3\}\}. \quad (10)$$

These configurations are selected as they have a similar or the same number of convolutional blocks to the optimal model configuration in [4], i.e.  $\{X, R\} = \{8, 3\}$ . The SISDR loss function [24] defined as

$$\mathcal{L}(\hat{\mathbf{s}}, \mathbf{s}_{dir}) := \frac{1}{C} \sum_{c=1}^C -10 \log_{10} \frac{\left\| \frac{\langle \hat{\mathbf{s}}_c, \mathbf{s}_{dir,c} \rangle \mathbf{s}_{dir,c}}{\|\mathbf{s}_{dir,c}\|^2} \right\|^2}{\left\| \hat{\mathbf{s}}_c - \frac{\langle \hat{\mathbf{s}}_c, \mathbf{s}_{dir,c} \rangle \mathbf{s}_{dir,c}}{\|\mathbf{s}_{dir,c}\|^2} \right\|^2} \quad (11)$$

is used to train the DTCN models. Permutation invariant training (PIT) is used to solve the speaker permutation problem [25].

Two GitHub repositories have been released in conjunction with this work. The first<sup>1</sup> is a Pytorch library for performing 1D de-

formable convolution. The second<sup>2</sup> is a model and *recipe* for reproducing our results with the DTCN model using the speechbrain [20] framework.

### 4.3. Evaluation Metrics

A number of metrics are used to evaluate the performance of the proposed DTCN models. SISDR and signal-to-distortion ratio (SDR) [26] are used to measure residual distortion in the signal. Perceptual evaluation of speech quality (PESQ) [27] and extended short-time objective intelligibility (ESTOI) [28] are used to measure speech quality and intelligibility, respectively. Speech-to-reverberation modulation energy ratio (SRMR) [29] is used to measure residual speech reverberation for the WHAMR corpus.

## 5. RESULTS

The results for various performance measures against each DTCN configuration's RF on the clean speech WSJ0-2Mix evaluation are shown in Fig. 4 where they are also compared against their corresponding TCN configurations. Note that the DTCN models have

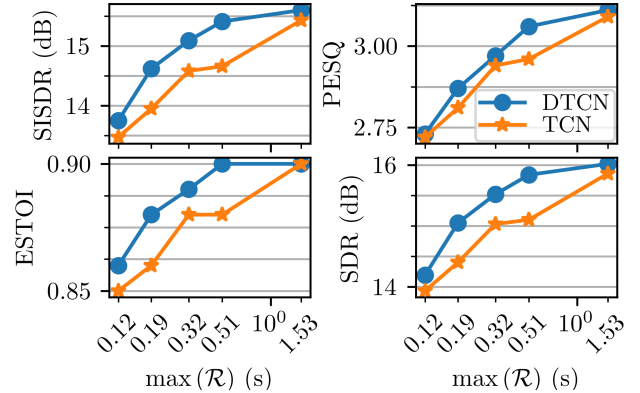


**Fig. 4:** Performance measures over RF for WSJ0-2Mix clean speech mixtures.

a small increase in number of parameters over the TCN models ( $\approx 6\%$ ) due to the offset estimation subnetworks. Performance improvements can be seen across all configurations but is more significant with the models which have a RF of 0.19s to 0.51s. The improvement in most metrics at the highest RF 1.53s is marginal and for the intelligibility metric ESTOI the performance is identical to the TCN.

Fig. 5 shows respective results for each DTCN configuration's RF against the performance measures on noisy reverberant WHAMR data. Note that SDR has been replaced by SRMR to provide a measure of reverberation. The DTCN again shows improvement over the TCN across all measures and model configurations. The performance also increases more consistently as the RF increases. The performance convergence seen on the clean speech mixtures in Fig. 4 at the largest RF,  $\mathcal{R} = 1.53$ s, is not seen in the results for the noisy reverberant data in Fig. 5. These findings suggest that deformable convolution is useful in particular for noisy reverberant data.

In Table 1 the proposed DTCN model is compared against other speech separation models in terms of size, efficiency and performance. Comparing for model size the proposed DTCN outperforms

<sup>1</sup>URL to dc1d pip repository: [github.com/jwr1995/dc1d](https://github.com/jwr1995/dc1d)

<sup>2</sup>URL to DTCN recipe: [github.com/jwr1995/DTCN](https://github.com/jwr1995/DTCN)

**Table 1:** Comparison of various DTCN models against other speech separation models with varying size and complexity. Dynamic Mixing is abbreviated to DM. Shared weights are abbreviated to SW. Computational efficiency is expressed in multiply-accumulate operations (MACs). Where possible, all MACs values have been estimated using *thop* [30] unless a citation is provided.

Model	WSJ0-2Mix		WHAMR		Model size	GMACs
	$\Delta$ SISDR	$\Delta$ SDR	$\Delta$ SISDR	$\Delta$ SDR		
Conv-TasNet [4]	15.3	15.6	9.2 [6]	-	5.1M	5.2
Conv-TasNet (w/o SC)	15.4	15.7	9.7	9.1	3.4M	3.5
SkiM-KS8 [31]	17.4	17.8	-	-	5.9M	4.9 [31]
Tiny-SepformerS-32 [12]	15.2	16.0	-	-	5.3M	-
SuDORM-RF 1.0x++ [11]	17	-	-	-	2.7M	2.3
SuDORM-RF 0.5x [11]	15.4	-	-	-	1.4M	<b>1.2</b>
FurcaNeXt [14]	-	18.4	-	-	51.4M	-
SepFormer+DM [5]	22.3	<b>22.4</b>	14.0	<b>13.0</b>	26M	69.6 [32]
QDPN+DM [23]	<b>23.6</b>	-	<b>14.4</b>	-	200M	-
DTCN (proposed)	15.6	15.9	10.2	9.3	3.6M	3.7
DTCN+DM (proposed)	17.2	17.4	11.1	10.3	3.6M	3.7
DTCN+SW (proposed)	15.0	15.3	10.0	9.3	<b>1.3M</b>	3.7
DTCN+SW+DM (proposed)	16.1	16.3	10.1	9.5	<b>1.3M</b>	3.7

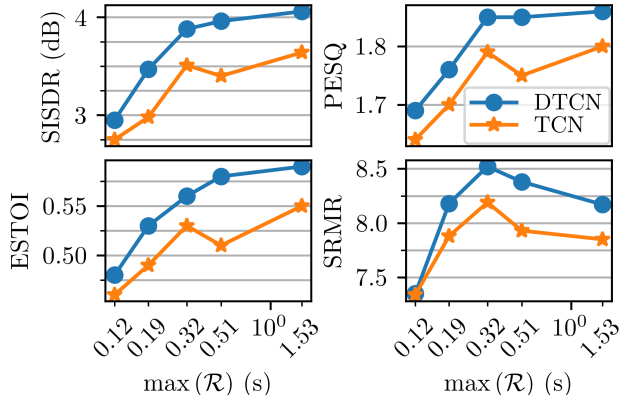


**Fig. 5:** Performance measures over RF for WHAMR noisy reverberant speech mixtures.

the larger convolutional Conv-TasNet model [4] and recurrent SkiM-KS8 model [31]. When DM is used in training, the DTCN outperforms the much larger convolutional SuDo-RM-RF 1.0x++ model [11]. Using SW reduces the model size by two thirds but is still able to give comparable performance to the SuDoRM-RF 0.5x model of similar size and much improved performance when DM is also used.

## 6. ANALYSIS

In the following the offset values of the best performing model configuration  $\{X, R\} = 8, 3$  are analysed with the aim to provide insight as to how temporal offsets  $\tau_{\ell, p}$  in (7), cf. also Fig. 2, behave relative to one another. The 2nd convolutional block of the 2nd repeat in the DTCN (i.e. the 10th block overall) was selected for analysis as it was found to have the highest average offset variance over the WHAMR evaluation set. The motivation for this choice is that it is assumed that blocks with offsets of larger variances are more indicative of the benefits of using deformable convolution. A correlation analysis was performed between each of three offset values averaged per utterance  $\bar{\tau}_p$ , corresponding to the three kernel weight positions. Fig. 6 shows scatter plots for the mean of the middle and outermost offsets denoted  $\bar{\tau}_2$  and  $\bar{\tau}_3$ , respectively, against the mean offset value of the first kernel sample point  $\bar{\tau}_1$  for every example in the evaluation set. A strong negative correlation ( $\rho = -0.99$ ) can be observed

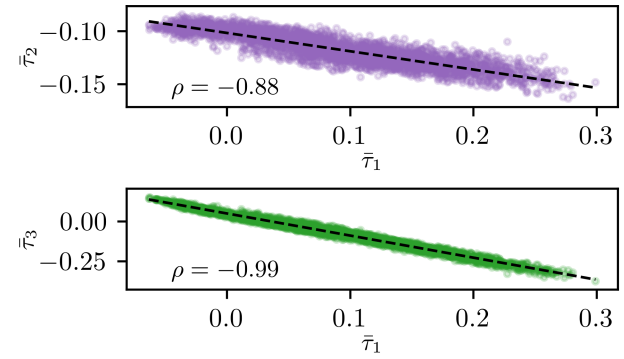


**Fig. 6:** Mean offset values  $\bar{\tau}_2$  (top) and  $\bar{\tau}_3$  (bottom) of the 10th convolutional block of the DTCN model plotted against the mean offset value of the first kernel weight  $\bar{\tau}_1$  for each example in the WHAMR evaluation set. Pearson correlation coefficients are denoted with  $\rho$ . Dashed black line indicates line of best fit.

between  $\bar{\tau}_1$  and  $\bar{\tau}_3$  indicating that the deformation is causing the RF of the kernel to shrink and grow more than shifting its focal point. A less strong negative correlation ( $\rho = -0.88$ ) was found between  $\bar{\tau}_1$  and  $\bar{\tau}_2$  indicating similar behaviour. The comparison of  $\bar{\tau}_2$  against  $\bar{\tau}_3$  is omitted from Fig 6 for brevity but these mean offset values were found to have a positive correlation of  $\rho = 0.81$ .

## 7. CONCLUSION

In this paper deformable convolution was proposed as a method to improve TCNs for noisy reverberant speech separation. It was shown that the DTCN model is particularly useful for noisy reverberant conditions as performance increases were less consistent in the case of anechoic speech separation with a sufficiently large receptive field. Using shared weights and dynamic mixing led to further performance improvements resulting in a small model size for the DTCN compared to other separation models which give comparable performance. Finally, it was shown that the DTCN offsets vary the size of the receptive field of convolutional blocks in the network relative to the input data.

## 8. REFERENCES

- [1] R. Haeb-Umbach, J. Heymann, L. Drude, S. Watanabe, M. Delcroix, and T. Nakatani, “Far-Field Automatic Speech Recognition,” *Proceedings of the IEEE*, vol. 109, no. 2, pp. 124–148, 2021.
- [2] J. Benesty, *An Introduction to Blind Source Separation of Speech Signals*, Kluwer Academic Publishers, USA, 2000.
- [3] Y. Shi and T. Hain, “Supervised Speaker Embedding Demixing in Two-Speaker Environment,” in *SLT Workshop 2021*, Jan 2021.
- [4] Y. Luo and N. Mesgarani, “Conv-TasNet: Surpassing ideal time-frequency magnitude masking for speech separation,” *IEEE/ACM Transactions on Audio, Speech, and Language Processing*, vol. 27, no. 8, pp. 1256–1266, 2019.
- [5] C. Subakan, M. Ravanelli, S. Cornell, M. Bronzi, and J. Zhong, “Attention is all you need in speech separation,” in *Interspeech 2021*, July 2021.
- [6] M. Maciejewski, G. Wichern, and J. Le Roux, “WHAMR!: Noisy and reverberant single-channel speech separation,” in *ICASSP 2020*, May 2020.
- [7] T. Cord-Landwehr, C. Boeddeker, T. von Neumann, C. Zorilla, R. Doddipatla, and R. Haeb-Umbach, “Monaural source separation: From anechoic to reverberant environments,” in *IWAENC 2022*, Sept. 2022.
- [8] T. Ochiai, M. Delcroix, R. Ikeshita, K. Kinoshita, T. Nakatani, and S. Araki, “Beam-TasNet: Time-domain audio separation network meets frequency-domain beamformer,” in *ICASSP 2020*, May 2020.
- [9] W. Ravenscroft, S. Goetze, and T. Hain, “Receptive Field Analysis of Temporal Convolutional Networks for Monaural Speech Dereverberation,” in *EUSIPCO 2022*, Aug. 2022.
- [10] M. Delcroix, T. Ochiai, K. Zmolikova, K. Kinoshita, N. Tawara, T. Nakatani, and S. Araki, “Improving speaker discrimination of target speech extraction with time-domain speakerbeam,” in *ICASSP 2020*, May 2020.
- [11] E. Tzinis, Z. Wang, X. Jiang, and P. Smaragdis, “Compute and memory efficient universal sound source separation,” *Journal of Signal Processing Systems*, vol. 94, no. 2, pp. 245–259, Feb 2022.
- [12] J. Luo, J. Wang, N. Cheng, E. Xiao, X. Zhang, and J. Xiao, “Tiny-sepformer: A tiny time-domain transformer network for speech separation,” in *Interspeech 2022*, Sept. 2022.
- [13] Y. Isik, J. Le Roux, Z. Chen, S. Watanabe, and J. R. Hershey, “Single-Channel Multi-Speaker Separation using Deep Clustering,” in *ICASSP 2016*, Sep. 2016.
- [14] L. Zhang, Z. Shi, J. Han, A. Shi, and D. Ma, “Furcanext: End-to-end monaural speech separation with dynamic gated dilated temporal convolutional networks,” in *MultiMedia Modeling*, Y. M. Ro, W.-H. Cheng, J. Kim, W.-T. Chu, P. Cui, J.-W. Choi, M.-C. Hu, and W. De Neve, Eds., Cham, 2020, Springer International Publishing.
- [15] W. Ravenscroft, S. Goetze, and T. Hain, “Utterance weighted multi-dilation temporal convolutional networks for monaural speech dereverberation,” in *IWAENC 2022*, Sept. 2022.
- [16] J. Dai, H. Qi, Y. Xiong, Y. Li, G. Zhang, H. Hu, and Y. Wei, “Deformable convolutional networks,” in *ICCV 2017*, Oct 2017.
- [17] D. Bhagya and M. Suchetha, “A 1-d deformable convolutional neural network for the quantitative analysis of capnographic sensor,” *IEEE Sensors Journal*, vol. 21, no. 5, pp. 6672–6678, 2021.
- [18] F. Chollet, “Xception: Deep learning with depthwise separable convolutions,” in *CVPR 2017*, July 2017.
- [19] N. Zeghidour and D. Grangier, “Wavesplit: End-to-end speech separation by speaker clustering,” *IEEE/ACM Transactions on Audio, Speech, and Language Processing*, vol. 29, pp. 2840–2849, 2021.
- [20] M. Ravanelli, T. Parcollet, P. Plantinga, A. Rouhe, S. Cornell, L. Lugosch, C. Subakan, N. Dawalatabad, A. Heba, J. Zhong, J. Chou, S. Yeh, S. Fu, C. Liao, E. Rastorgueva, F. Grondin, W. Aris, H. Na, Y. Gao, R. D. Mori, and Y. Bengio, “SpeechBrain: A general-purpose speech toolkit,” 2021, arXiv:2106.04624.
- [21] W. Ravenscroft, S. Goetze, and T. Hain, “Att-TasNet: Attending to Encodings in Time-Domain Audio Speech Separation of Noisy, Reverberant Speech Mixtures,” *Frontiers in Signal Processing*, vol. 2, 2022.
- [22] J. R. Hershey, Z. Chen, J. Le Roux, and S. Watanabe, “Deep clustering: Discriminative embeddings for segmentation and separation,” in *ICASSP 2016*, Mar. 2016.
- [23] J. Rixen and M. Renz, “QDPN - Quasi-dual-path Network for single-channel Speech Separation,” in *Interspeech 2022*, Sept. 2022.
- [24] Y. Luo and N. Mesgarani, “TasNet: Time-domain audio separation network for real-time, single-channel speech separation,” in *ICASSP 2018*, Apr. 2018.
- [25] M. Kolbaek, D. Yu, Z.-H. Tan, J. Jensen, M. Kolbaek, D. Yu, Z.-H. Tan, and J. Jensen, “Multitalker speech separation with utterance-level permutation invariant training of deep recurrent neural networks,” *IEEE/ACM Trans. Audio, Speech and Lang. Proc.*, vol. 25, no. 10, pp. 1901–1913, oct 2017.
- [26] J. Le Roux, S. Wisdom, H. Erdogan, and J. R. Hershey, “SDR – Half-baked or Well Done?,” in *ICASSP 2019*, May 2019.
- [27] A. Rix, J. Beerends, M. Hollier, and A. Hekstra, “Perceptual evaluation of speech quality (PESQ)-a new method for speech quality assessment of telephone networks and codecs,” in *ICASSP 2001*, May 2001.
- [28] J. Jensen and C. H. Taal, “An algorithm for predicting the intelligibility of speech masked by modulated noise maskers,” *IEEE/ACM Transactions on Audio, Speech, and Language Processing*, vol. 24, no. 11, pp. 2009–2022, 2016.
- [29] T. H. Falk, C. Zheng, and W.-Y. Chan, “A non-intrusive quality and intelligibility measure of reverberant and dereverberated speech,” *IEEE Transactions on Audio, Speech, and Language Processing*, vol. 18, no. 7, pp. 1766–1774, 2010.
- [30] “Thop: Pytorch-opcounter,” <https://pypi.org/project/thop/>, Accessed: 19-10-2022.
- [31] C. Li, L. Yang, W. Wang, and Y. Qian, “Skim: Skipping memory lstm for low-latency real-time continuous speech separation,” in *ICASSP 2022*, May 2022.
- [32] C. Subakan, M. Ravanelli, S. Cornell, F. Lepoutre, and F. Grondin, “Resource-efficient separation transformer,” 2022, arXiv:2206.09507.